An Ultrasonic Sensor for Distance Measurement in Automotive Applications

Alessio Carullo and Marco Parvis, *Senior Member, IEEE*

Abstract—**This paper describes an ultrasonic sensor that is able to measure the distance from the ground of selected points of a motor vehicle. The sensor is based on the measurement of the time of flight of an ultrasonic pulse, which is reflected by the ground. A constrained optimization technique is employed to obtain reflected pulses that are easily detectable by means of a threshold comparator. Such a technique, which takes the frequency response of the ultrasonic transducers into account, allows a sub-wavelength detection to be obtained. Experimental tests, performed with a 40 kHz piezoelectric-transducer based sensor, showed a standard uncertainty of 1 mm at rest or at low speeds; the sensor still works at speeds of up to 30 m/s, although at higher uncertainty. The sensor is composed of only low cost components, thus being apt for first car equipment in many cases, and is able to self-adapt to different conditions in order to give the best results.**

Index Terms—**Acoustic devices, distance measurement, intelligent sensors.**

I. INTRODUCTION

THE DEVELOPMENT of "smart cars" requires new sensors that are able to measure distances in the range of a few centimeters to a few meters. Parking aids, as well as intelligent suspensions and headlight leveling, are some examples of features that require a distance measurement to be performed with contactless sensors. Several different physical principles can be employed to measure the distance [1] [2], but price limits greatly restrict the actual choices.

An interesting possibility, which has been investigated by several authors, is the use of ultrasonic sensors based on the well known time of flight technique [3]–[8]. Such sensors are reasonably cheap and work for ranges of up to a few meters, even though problems arise regarding both their accuracy and their behavior in noisy open-air conditions.

In this paper the authors describe a low-cost ultrasonic distance meter that performs contactless measurement of the height from the ground of a vehicle body. The sensor performance is better than many commercial devices, thanks to the possibility the sensor has of evaluating the environmental conditions and then self-adapting to these conditions.

The sensor has been designed in order to satisfy typical requirements in the automotive field: measured distance in the range of 0.1–0.3 m and standard uncertainty of 1 mm in the temperature range of 0 °C to 40 °C. Measurements of distances

up to 1 m and in a wider temperature ranges are possible even though at higher uncertainty.

II. OPERATING PRINCIPLE

The distance from the ground of a point of a vehicle body is computed as

$$D = k \cdot T_f \cdot V_s \tag{1}$$

where

T_f time of flight of an ultrasonic pulse, i.e., the time the pulse takes to cover the distance D;

k constant close to 0.5, which depends on the sensor geometry;

V_s velocity of sound in air.

The ultrasonic pulse is generated using a piezoelectric transducer and the echo reflected by the ground is received by another piezoelectric transducer. The two transducers are mounted close to each other to make up the measuring head. The uncertainty contribution due to the constant k can be made negligible by means of a sensor calibration after mounting the measuring head.

As the measured quantities T_f and V_s can be considered uncorrelated, the standard uncertainty $u(D)$ of the measured distance can be obtained from equation (1) as [9]

$$u(D) = \sqrt{(k \cdot T_f)^2 \cdot u^2(V_s) + (k \cdot V_s)^2 \cdot u^2(T_f)} \tag{2}$$

where $u(V_s)$ and $u(T_f)$ are the standard uncertainties of the velocity of sound and of the time of flight.

The velocity of sound in air depends on the temperature θ and, to a lesser extent, on the air humidity h

$$V_s = f(\theta, h) \tag{3}$$

therefore, (2) becomes

$$u(D) = \sqrt{(k \cdot T_f)^2 \cdot \left[\left(\frac{\partial f}{\partial \theta}\right)^2 \cdot u^2(\theta) + \left(\frac{\partial f}{\partial h}\right)^2 \cdot u^2(h)\right] + (k \cdot V_s)^2 \cdot u^2(T_f)}. \tag{4}$$

If the humidity is considered a random variable uniformly distributed in the range of 10%RH to 90%RH, its effect on the velocity of sound is of about 0.15% at 20 °C. This leads to a standard uncertainty contribution of about 0.3 mm for a distance range of 0.3 m, hence a humidity sensor is not necessary.
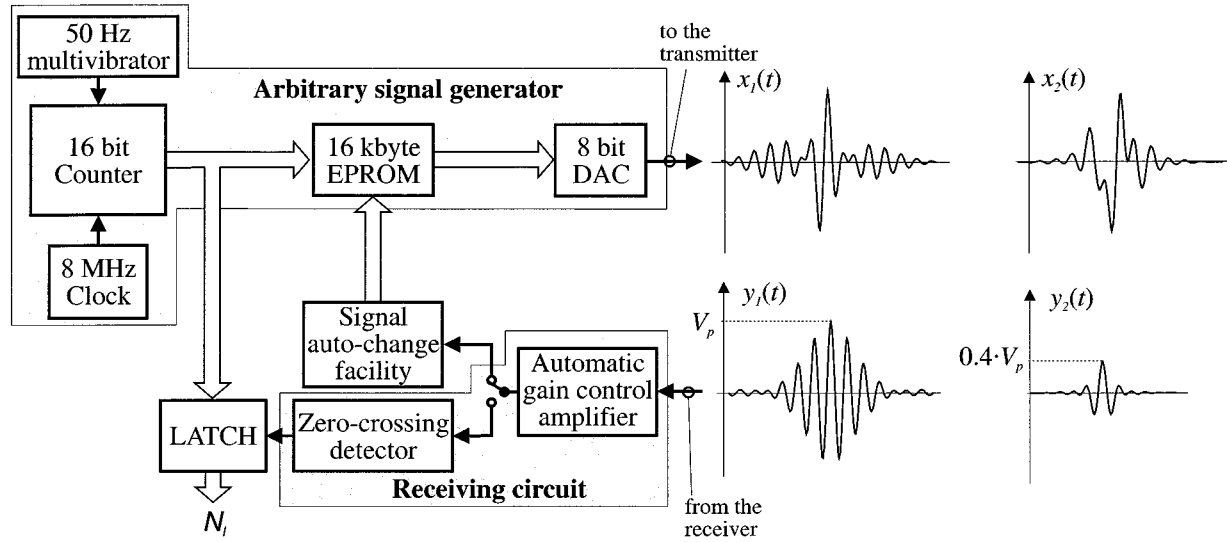
Fig. 1. Ultrasonic sensor arrangement and two examples of stimulating signals and expected echoes. The stronger echo $y_1(t)$ (peak amplitude V_p) is obtained by stimulating the transmitter with the signal $x_1(t)$; the narrower and weaker echo $y_2(t)$ (peak amplitude $0.4 \cdot V_p$), which is suitable in low noise conditions, is obtained by employing the stimulus signal $x_2(t)$.

The velocity of sound in air depends on the temperature according to the approximated equation

$$V_s \approx 20.055 \cdot \sqrt{T} \qquad (5)$$

where T is the absolute temperature, which is measured in kelvin.

Velocity-of-sound changes in the range of 330–360 m/s have to, therefore, be expected for temperature changes in the range of 0–40 °C. Such an effect must be taken into account in the determination of the distance, hence a temperature sensor is required.

Another phenomenon that affects the uncertainty of the measured distance is the car speed, which has the same effect of the component of the wind that flows perpendicularly to the path of the ultrasonic pulse. Such effect consists in an increasing of the pulse path and, in turn, of the measured distance. As the maximum car-speed is of the order of 10% of the velocity of the sound, the distance error due to a car speed V_w can be approximately estimated as

$$\frac{\Delta D}{D} \approx \frac{1}{2} \cdot \left(\frac{V_w}{V_s} \right)^2. \qquad (6)$$

For a car speed of 33 m/s (about 120 km/h), the distance error at 0 °C ($V_s \approx 330$ m/s) is of about 0.5%. One should note that this error could be easily corrected by the knowledge of the car speed.

Distance measurement in the range of 0.1 m to 0.3 m requires the measurement of time of flights in the range of 0.5–2 ms.

The required distance standard uncertainty of 1 mm can be achieved by measuring the time of flight with a standard uncertainty of 2.5 μs, the temperature with a standard uncertainty of 1 °C, and avoiding the use of a humidity sensor.

Ultrasonic signals with frequencies in the range of 30 kHz to 5 MHz can be used to generate the pulse. Higher frequen-

cies might be preferable since they imply lower wavelengths and thus a potentially better resolution, but the sound attenuation in the air dramatically increases as the frequency increases. In addition, higher frequencies require both costly transducers and fast electronic devices, therefore preventing a low-cost arrangement to be obtained. Lower frequencies have the advantage of low-scattering problems and can be obtained with low cost transducers, but the wavelength in the air is several millimeters, thus requiring special care in order to obtain measurement uncertainties that are lower than the wavelength.

Several approaches have been investigated to obtain sub-wavelength uncertainties [3]–[8] with rather good results, but the proposed solutions generally require the use of some form of digital processing of the acquired data, thus increasing the sensor cost. The sensor implementation that is proposed by the authors and described in the following section avoids the use of such a digital processing in order to keep the cost very low.

III. Sensor Implementation

A. Time Of Flight Measurement

The sensor employs commercial 40 kHz piezoelectric resonant transducers to generate the ultrasonic pulse. Such transducers, which are commonly employed in anti-thief systems, are readily available in waterproof containers for a cost of about one dollar.

The period of the generated signal is 25 μs, which corresponds to a wavelength of about 9 mm at 20 °C. A subwavelength detection is therefore necessary in order to obtain the required uncertainty.

The required T_f standard uncertainty of 2.5 μs is achieved with a costless arrangement, which is basically composed of an arbitrary signal generator and a zero-crossing detector.

The signal generator (see Fig. 1) is composed of a 16 kbyte EPROM, which contains the samples corresponding to the sig-

nals to be generated, a 16 bit counter, that is used to scan the EPROM, and an 8 bit digital-to-analog converter (DAC) that feeds the transmitting piezoelectric transducer.

The zero-crossing detector is made up of two threshold detectors. A first detector, whose threshold is a portion of the received-signal peak, enables a second detector that compares the received signal with respect to the reference ground. This allows the detection in the signal region at maximum slope to be obtained, thus minimizing noise effects.

The stimulus signals that are stored in the EPROM are specially designed to obtain echoes that are narrow enough to prevent the first threshold detector firing on different periods of the echo. Such special signals are designed by means of a constrained optimization procedure, which is based on the minimization of the echo energy while constraining the echo peak to reach a fixed value. The optimum driving signal $\mathbf{X}_{opt}(f)$ that permits to receive the narrowest echo $\mathbf{Y}_p(f)$ of fixed amplitude is obtained by solving the following equations

$$\mathbf{X}_{opt}(f) = -\frac{1}{2}\lambda_1 \cdot \frac{\mathbf{H}^*(f)}{|\mathbf{H}(f)|^2 + \lambda_2} \qquad (7)$$

$$\mathbf{Y}_p(f) = -\frac{1}{2}\lambda_1 \cdot \frac{|\mathbf{H}(f)|^2}{|\mathbf{H}(f)|^2 + \lambda_2} \qquad (8)$$

where $\mathbf{H}(f)$ is the frequency response of the transmission channel, which is made up of transmitter, propagation medium and receiver, while the parameters λ_1 and λ_2 are the Lagrange multipliers, which are computed by numerically solving the system of nonlinear equations

$$-\frac{\lambda_1}{2} \cdot \int_{-\infty}^{\infty} \frac{|\mathbf{H}(f)|^2}{|\mathbf{H}(f)|^2 + \lambda_2}\, df = \alpha \cdot y_{p\max}$$

$$\frac{\lambda_1^2}{4} \cdot \int_{-\infty}^{\infty} \frac{|\mathbf{H}(f)|^2}{[|\mathbf{H}(f)|^2 + \lambda_2]^2}\, df = W \qquad (9)$$

where W is the maximum permitted energy of the stimulating signal, and $\alpha \cdot y_{p\max}$ ($\alpha \leq 1$) is the required peak amplitude of the echo. A detailed description of the optimization procedure can be found in [10].

The optimization result depends on the chosen echo amplitude: the lower the required amplitude, the narrower the echo and, thus, the lower the misfiring probability for a certain relative noise amplitude. Two examples of stimulus signals $x(t)$ and of the corresponding expected echoes $y(t)$ are shown in Fig. 1. The best signal to employ under any condition therefore depends on the actual amount of noise [11].

The sensor contains a simple noise measuring system that estimates the actual noise by monitoring the input signal during echo-free intervals. The noise measuring system output is used to switch between three optimal signals, which are tailored for good results in low, medium, and high noise conditions, as described in [11].

In addition, the echo amplitude mainly depends on the reflectivity of the ground and on its distance. Such effects are minimized by employing an automatic gain control amplifier in the receiving circuit so that the echo amplitude is maintained at a fixed value. This allows a fixed threshold of the first detector to
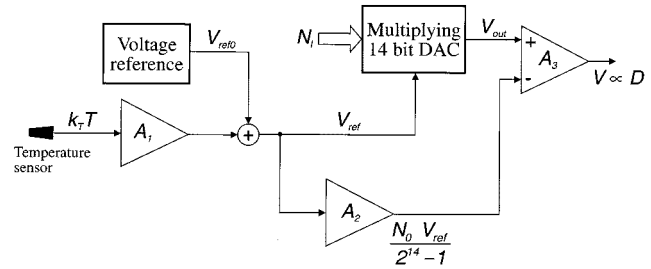

Fig. 2. Temperature compensation circuit.

be employed. The output of the zero-crossing detector is used to drive a latch that freezes the counter output at the value reached at the echo arrival time. If a new echo is not detected, the latch output is not updated, thus avoiding meaningless measurements. The value that is actually latched is the sum of the counts corresponding to the time of flight and of a known fixed value N_0, which depends on the way the stimulating signals are stored in the EPROM and on the threshold level of the first detector.

The time base of the system runs at 8 MHz, therefore the time resolution is of 125 ns and the maximum measurable time of flight is of about 8 ms, which corresponds to a distance greater than 1 m. A 50 Hz multivibrator restarts the counter providing a reading every 20 ms.

B. Temperature Measurement and Distance Estimation

The measurement of the air temperature is carried out by using a solid state sensor that has a sensitivity k_T of 10 mV/°C. The sensor is mounted inside the measuring head and has an uncalibrated error of less than 1 °C.

The distance is computed by the simple analog circuit shown in Fig. 2. A low-cost multiplying 14 bit DAC is fed with the latched counter output N_l to produce a voltage V_{out} that is proportional to the time of flight:

$$V_{\text{out}} = V_{ref} \cdot \frac{N_l}{2^{14} - 1}. \qquad (10)$$

The 14 DAC digital inputs are connected to the most significant bits of the counter, so that the less significant bit corresponds to a time interval of 0.5 μs. The DAC nonlinearity affects negligibly the overall measurement uncertainty.

The DAC voltage reference V_{ref} is obtained by summing a fixed reference V_{ref0} to a calibrated fraction of the voltage produced by the temperature sensor, thus producing a voltage proportional to the temperature according to the formula

$$V_{ref} = V_{ref0} + A_1 \cdot k_T \cdot T. \qquad (11)$$

By adjusting the values of the coefficient A_1, it is possible to obtain a V_{ref} change with the temperature that partially compensates for the velocity of the sound change. The compensation is not complete, since the velocity of sound varies with the square root of the temperature and the reference voltage changes linearly with the temperature. The residual temperature effect has been analytically estimated by comparing the effects of the velocity of the sound in air and of the temperature-dependent
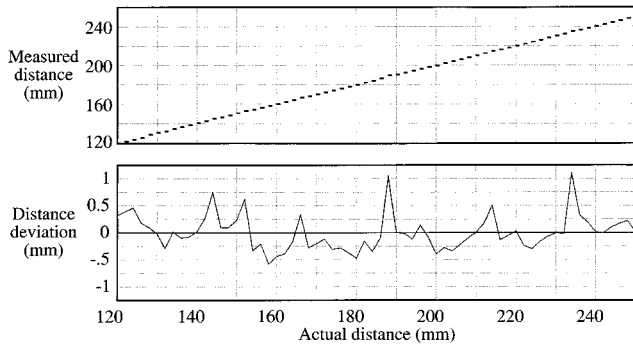
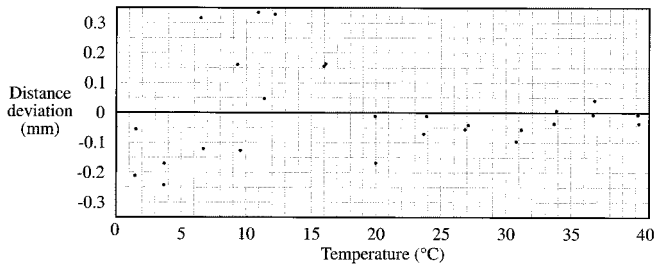Fig. 3.   Sensor linearity with respect to distance.

Fig. 4.   Temperature effect on a fixed measured distance.

reference voltage on the output voltage V. The expected temperature effect is of less than $\pm 0.03\%$ (about ± 0.1 mm for a measured distance of 0.3 m) in the range of 0 °C to 40 °C. The same effect becomes of about $\pm 0.1\%$ (± 0.3 mm for $D = 0.3$ m) if a temperature range of -20 °C to 70 °C is considered, which is a reasonable temperature range of automotive sensors.

The analog circuit is completed by the operational amplifiers A_2 and A_3 that subtract from the output a voltage corresponding to the fixed code N_0, thus generating a voltage that is only proportional to the distance.

The latched digital output is available for further digital processing [8] along with an optional digital temperature value provided by an 8 bit analog to digital converter. The sensor calibration can be obtained by operating on gain and zero trimmers while moving the sensor head between two known distances.

IV. EXPERIMENTAL RESULTS

A. Laboratory Tests

The sensor has been initially calibrated and tested in laboratory for distances in the range of 0.1–0.6 m and for temperatures in the range of 0–40 °C. The experimental standard deviation of the linearity with respect to the distance has been found to be of 0.3 mm (see Fig. 3), while the temperature effect produces a standard deviation of less than 0.2 mm (see Fig. 4) as expected.

The air turbulence effect has been investigated for speeds of up to 10 m/s by moving the air with a variable-speed fan; the noise measurement system and the signal auto-change facility have been tested by artificially generating an ultrasonic noise with an additional piezoelectric transducer. The overall standard uncertainty, when the distance is measured from a flat surface,
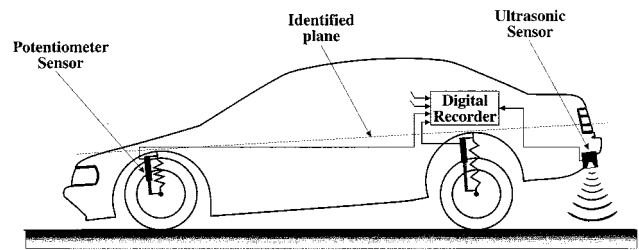

Fig. 5.   Sensor arrangement on the car that has been used for the tests.

in the absence of acoustic noise, for temperatures in the range of 0–40 °C and distances in the range of 0.1–0.6 m, is better than 1 mm.

B. Field Tests

The measuring head has been mounted onto the back of a car (see Fig. 5), which has been equipped with four potentiometer sensors to measure the spring heights during the car movement. A portable digital recorder has been used to record the ultrasonic sensor and the potentiometer outputs. Tests have been performed at different speeds on asphalt and rough ground.

The four potentiometer outputs have been used to compute a distance reference value to be compared with the ultrasonic measured distance. The end spring heights, which have been estimated by adding the tire deformations to the spring heights measured by the potentiometers, have been used to identify the plane of the vehicle body. The distance reference value that corresponds to the distance the ultrasonic sensor should produce has been determined by putting the measuring head coordinates into the identified plane equation.

The results of one of the tests is shown in Fig. 6, where the thicker line represents the ultrasonic sensor output while the thinner line is the computed output. The two traces are in good agreement except for a few time intervals, where road irregularities are present. The effect of such irregularities is a different distance sensed by the ultrasonic sensor, which is installed at the center of the vehicle body, and by the potentiometer sensors that are allocated at the vehicle sides.

V. CONCLUSION

A low-cost distance sensor is described in this paper that is able to self-adapt to the environmental conditions. The sensor contains a noise measurement system and an auto-change facility of the signal that is used to drive the transmitter, thus producing the best accuracy under different conditions.

Tests have been performed in real driving conditions and have shown a regular behavior of the sensor under all typical driving maneuvers for speeds of up to 33 m/s (120 km/h). The sensor features a simple and costless analog processing of the signal without employing microprocessors.

Despite its simplicity and low-cost, the sensor allows resolutions of better than 1 mm to be obtained in quiet conditions. The sensor output is updated every 20 ms, and an additional digital output allows an easy implementation of smoothing techniques by means of the car computing system. The obtained measurements are accurate enough for headlight leveling as well as for
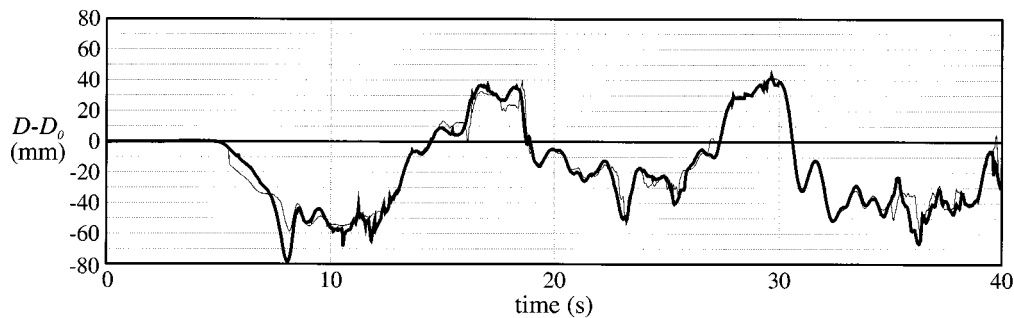
Fig. 6. Example of traces during a typical test (the thick line is the ultrasonic sensor output, while the thin line is the computed output). D_0 is the height of the measuring head at rest.

giving an important piece of information to active suspension systems.

REFERENCES

[1] Honeywell Sensing and Control Catalog. (2000) Series 940-942 Ultrasonic Sensors. [Online]. Available: www.honeywell.ca/sensing/.
[2] Philtec Product Data Sheet. (2000) Series D6-D171 Fiberoptic Displacement Sensors. [Online]. Available: http://www.philtec.com/datasheets.htm.
[3] M. Parrilla, J. J. Anaya, and C. Fritsch, "Digital signal processing techniques for high accuracy ultrasonic range measurements," *IEEE Trans. Instrum. Meas.*, vol. 40, pp. 759–763, Aug. 1991.
[4] D. Marioli, C. Narduzzi, C. Offelli, D. Petri, E. Sardini, and A. Taroni, "Digital time-of-flight measurement for ultrasonic sensors," *IEEE Trans. Instrum. Meas.*, vol. 41, pp. 93–97, Feb. 1992.
[5] C. Cai and P. L. Regtien, "Accurate digital time-of-flight measurement using self-interference," *IEEE Trans. Instrum. Meas.*, vol. 42, pp. 990–994, Dec. 1993.
[6] F. Gueuning, M. Varlan, C. Eugène, and P. Dupuis, "Accurate distance measurement by an autonomous ultrasonic system combining time-of-flight and phase-shift methods," in *Proc. IMTC*, vol. I, Brussels, Belgium, June 4–6, 1996, pp. 399–404.
[7] G. Andria, F. Attivissimo, and A. Lanzolla, "Digital measuring techniques for high accuracy ultrasonic sensor application," in *Proc. IMTC*, vol. II, St. Paul, MN, May 18–21, 1998, pp. 1056–1061.
[8] A. Carullo, F. Ferraris, S. Graziani, U. Grimaldi, and M. Parvis, "Ultrasonic distance sensor improvement using a two-level neural network," *IEEE Trans. Instrum. Meas.*, vol. 45, pp. 677–682, April 1996.
[9] ENV 13 005, "Guide to the expression of uncertainty in measurement,", May 1999.
[10] U. Grimaldi and M. Parvis, "Enhancing ultrasonic sensor performance by optimization of the driving signal," *Measurement*, vol. 14, pp. 219–228, 1995.
[11] U. Grimaldi and M. Parvis, "Noise-tolerant ultrasonic distance sensor based on a multiple driving approach," *Measurement*, vol. 15, pp. 33–41, 1995.

Alessio Carullo was born in Italy in 1966. He received the M.S. degree in electronic engineering in 1992 from Politecnico di Torino, Torino, Italy, and the Ph.D. degree in electronic instrumentation in 1997 from the Università di Brescia, Italy.

Currently, he is with the Dipartimento di Elettronica of Politecnico di Torino where, since 1998, he has been responsible for the Department calibration-laboratory. His main fields of interest are the development and characterization of intelligent instrumentation and of systems for chemical measurements and for power measurements in distorted environment. He is with the working group SIT-GE/GL1 for the validation of automatic calibration systems.

Marco Parvis (M'97–SM'01) was born in Italy in 1958. He received the M.S. degree in electrical engineering in 1982 from the Politecnico di Torino, Torino, Italy, and the Ph.D. degree in metrology in 1987.

He is now a Professor of electronic measurements at the Politecnico di Torino. His main fields of interest are intelligent instrumentation, signal processing, and biomedical measurements. He is working now on new sensors for mechanical and chemical quantities, and on the development of distributed measuring systems.